

Fig. (1). Schematic diagrams for the processes contributing to strangeness production in ep scattering: (a) direct production from the strange sea, (b) BGF, (c) heavy hadron decays and (d) fragmentation. The diagrams relevant for K^0 production are shown.

The K_s^0 mesons and Λ baryons² are measured by the kinematic reconstruction of their decays $K_s^0 \rightarrow \pi^+ \pi^-$ and $\Lambda \rightarrow p \pi^-$, respectively. The number of K_s^0 mesons and Λ baryons is obtained by fitting the invariant mass spectra with the sum of a signal and background function. For the signal function the skewed t-student function is used while the background shape is described by a threshold function with exponential damping. In total approximately 290000 K_s^0 mesons and 7000 $\Lambda(\bar{\Lambda})$ baryons are reconstructed in the phase space given in Table 1. The fitted K_s^0 and Λ masses agree with the world average [4].

Table 1. Phase Space Regions Explored in the Analyses of K_s^0 and Λ Production, Respectively

DIS Kinematics	
K_s^0	$7 < Q^2 < 100 \text{ GeV}^2, 0.1 < y < 0.6$
Λ	$145 < Q^2 < 20000 \text{ GeV}^2, 0.2 < y < 0.6$
Hadron Kinematics	
K_s^0	$0.5 < p_T < 3.5 \text{ GeV}, -1.3 < \eta < 1.3$
Λ	$p_T > 0.3 \text{ GeV}, -1.5 < \eta < 1.5$

3. RESULTS AND DISCUSSION

3.1. Inclusive Cross Sections

The visible inclusive production cross sections σ_{vis} measured in the kinematic region defined in Table 1, are $\sigma_{vis}(ep \rightarrow eK_s^0 X) = 10.66 \pm 0.02(stat.)_{-8.5}^{+9.4}(syst.)nb$, $\sigma_{vis}(ep \rightarrow e\Lambda X) = 144.7 \pm 0.04(stat.)_{-8.5}^{+9.4}(syst.)pb$ using a strangeness suppression factor of $\lambda_s = 0.286$ the models RAPGAP [5] and DJANGO [6] predict K_s^0 cross sections

of 10.93 nb and 9.88 nb, respectively, in reasonable agreement with the measurement. The cross section predictions for $\Lambda + \bar{\Lambda}$ production from the MEPS and CDM [7] models are shown in Table 2 for two values of the strangeness suppression parameter λ_s . The measured inclusive $\Lambda + \bar{\Lambda}$ cross section is close to the CDM prediction with $\lambda_s = 0.22$ and to the MEPS prediction with $\lambda_s = 0.286$.

Table 2. Monte Carlo Predictions for Different Settings of the Strangeness Suppression Factor λ_s

	$\lambda_s = 0.220$	$\lambda_s = 0.286$
$\sigma_{vis}(ep \rightarrow e[\Lambda + \bar{\Lambda}]X)$ CDM	136 pb	161 pb
$\sigma_{vis}(ep \rightarrow e[\Lambda + \bar{\Lambda}]X)$ MEPS	120 pb	144 pb

3.2. Differential Cross Sections

Differential cross sections of K_s^0 and Λ production are shown in Figs. (2a, b, 3a) as a function of Q^2 , and as a function of the kinematic variable of the neutral strange hadrons in the laboratory frame, η along with the predictions of the MEPS and CDM models. The cross sections fall rapidly as Q^2 grows. The figures also include the ratios of predicted to measured cross sections for a better shape comparison. Apart from small normalisation differences the models describe the shapes of the measured cross sections as a function of Q^2 and η reasonably well.

3.3. Ratio of K_s^0 Production to Charged Particle Production

By normalising the K_s^0 production cross section to the cross section of charged particle production many model dependent uncertainties, like the cross section dependence on proton PDFs, cancel thus enhancing the sensitivity to details

²Unless otherwise noted, charge conjugate states are always implied.

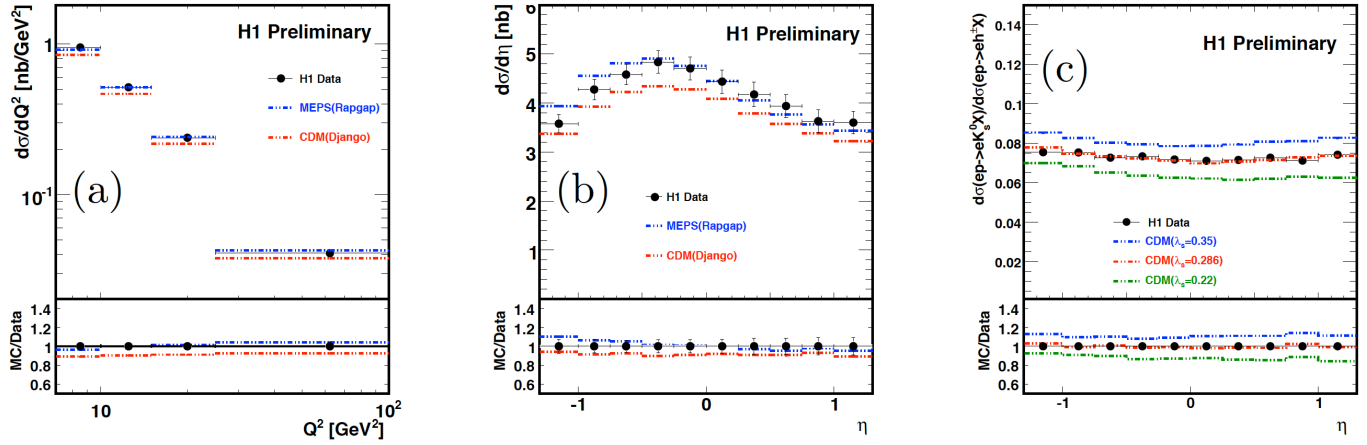


Fig. (2). Differential K_s^0 production cross sections as a function of (a) the photon virtuality squared Q^2 , (b) its pseudorapidity η and (c) ratio of K_s^0 to charged particle production as a function of η in comparison to RAPGAP (MEPS) and DJANGO (CDM). The inner (outer) error bars show the statistical (total) errors. The ratios “MC/Data” are shown for the different Monte Carlo predictions. For comparison, the data points are put to one.

of the fragmentation process. In Fig. (2c) the ratio of K_s^0 production to the cross section charged particle production is shown as a function of η in comparison to the expectations from DJANGO using three different values of λ_s ranging from 0.220 to 0.35. The ratio in η is well described by the model in shape and a high sensitivity on λ_s is observed in the absolute value of this ratio, demonstrating the clear potential of using this ratio for extracting the strangeness suppression factor λ_s .

3.4. Λ Production to DIS Cross Section Ratio

In Fig. (3b) the ratio of Λ production to DIS cross section is shown as a function of Q^2 in comparison to the expectations from RAPGAP and DJANGO both using $\lambda_s = 0.286$ and $\lambda_s = 0.220$. The DJANGO prediction

with $\lambda_s = 0.286$ yields the worst description of the data by overshooting them significantly independent of Q^2 . For the same strangeness suppression factor also RAPGAP tends to yield ratios larger than observed in data for $Q^2 < 200 \text{ GeV}^2$. The best description is provided by DJANGO using $\lambda_s = 0.220$.

3.5. $\Lambda - \bar{\Lambda}$ Asymmetries

The $\Lambda - \bar{\Lambda}$ asymmetry is defined as:

$$A_\Lambda = \frac{\sigma_{\text{vis}}(ep \rightarrow e\Lambda X) - \sigma_{\text{vis}}(ep \rightarrow e\bar{\Lambda} X)}{\sigma_{\text{vis}}(ep \rightarrow e\Lambda X) + \sigma_{\text{vis}}(ep \rightarrow e\bar{\Lambda} X)} \quad (1)$$

This observable could shed light on the mechanism of baryon number transfer in ep scattering. A significant positive asymmetry would be an indication for the baryon

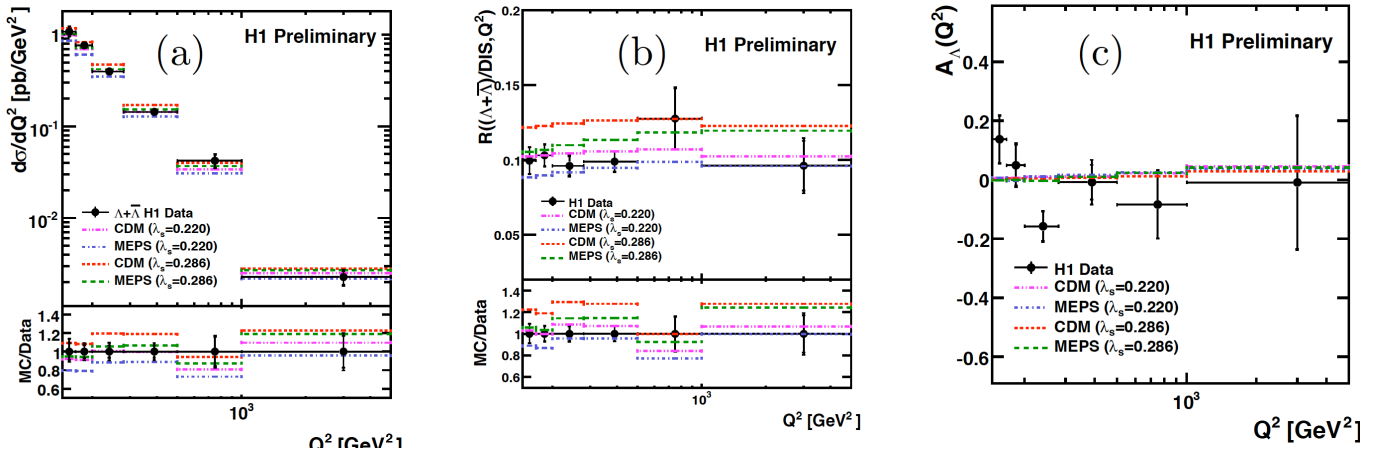


Fig. (3). The Q^2 dependence of (a) differential Λ production cross section, (b) ratio $R(\text{DIS})$ of Λ production to DIS cross section and (c) asymmetry A_Λ in comparison to RAPGAP (MEPS) and DJANGO (CDM) with two different values of λ_s . The inner (outer) error bars show the statistical (total) errors. The “MC/Data” ratios are shown for different Monte Carlo predictions. For the ratios the data points are put at one for comparison.

number transfer from the proton to the Λ baryon. If present such an effect should be more pronounced in the positive η region in the laboratory frame. For the kinematic region defined in table 1 the asymmetry is measured to be

$$A_\Lambda = 0.002 \pm 0.022(\text{stat.}) \pm 0.018(\text{syst.}).$$

In Fig. (3c) the asymmetry A_Λ is shown as a function of Q^2 . The data show no evidence for a non-vanishing asymmetry in the phase space region investigated.

4. CONCLUSIONS

This paper presents a study of inclusive production of K_s^0 and Λ in DIS at low Q^2 and high Q^2 measured with the H1 detector at HERA. The cross sections of K_s^0 and Λ production are measured as a function of the DIS kinematic variable Q^2 and of strange hadron production variables in the laboratory frame. In addition results on the ratio of K_s^0 production cross section to the charged particle cross section, the Λ production to DIS cross section ratio and the $\Lambda - \bar{\Lambda}$ asymmetry are presented. The measurements are compared to model predictions of DJANGO, based on the colour-dipole model (CDM) and RAPGAP based on DGLAP matrix element calculations supplemented with parton showers (MEPS). Within the uncertainties both models provide a reasonable description of the data. The sensitivity of the ratio of K_s^0 to charged particle production cross sections on the strangeness suppression factor λ_s is demonstrated, however, a detailed understanding of concurrent processes of K_s^0 production is mandatory prior to the determination of λ_s . The measured visible Λ cross section is found to be

described best by the CDM using $\lambda_s = 0.220$ and the MEPS model using $\lambda_s = 0.286$. When investigating the Λ production to DIS cross section ratio the best agreement is observed for the CDM with $\lambda_s = 0.220$. The $\Lambda - \bar{\Lambda}$ asymmetry is found to be consistent with zero.

CONFLICT OF INTEREST

The authors confirm that this article content has no conflicts of interest.

ACKNOWLEDGEMENTS

Declared none.

REFERENCES

- [1] Sjöstrand T. High-energy physics event generation with PYTHIA 5.7 and JETSET 7.4. *Comput Phys Commun* 1994; 82: 74. JETSET version 7.4 is used.
- [2] (a). Sjöstrand T. The Lund Monte Carlo for jet fragmentation and E+ E- Physics: Jetset Version 6.2. *Comput. Phys Commun* 1986; 39: 347. (b). Sjöstrand T, Bengtsson M. The Lund Monte Carlo for jet fragmentation and E+ E- physics. Jetset Version 6.3: An Update. *Comput Phys Commun* 1987; 43: 367. (c). Andersson B, *et al.* Parton fragmentation and string dynamics. *Phys Rept* 1983; 97: 31.
- [3] (a). Abt I, *et al.* [H1 Collaboration]. The H1 detector at HERA. *Nucl Instrum Meth A* 1997; 386: 310. (b). Abt I, *et al.* [H1 Collaboration]. The tracking, calorimeter and muon detectors of the H1 experiment at HERA. *Nucl Instrum Meth A* 1997; 386: 348.
- [4] Nakamura K, *et al.* (Particle Data Group). *J Phys G* 2010; 37: 075021.
- [5] Jung H, Hard diffractive scattering in high-energy e p collisions and the Monte Carlo generator RAPGAP. *Comp Phys Commun* 1995; 86: 147.
- [6] Schuler GA, Siesberger H. DJANGO. *Proceedings of Physics at HERA*. Buchmüller W, Ingelman G, editors. DESY, Hamburg 1992; 1419.
- [7] (a). Andersson B, *et al.* Coherence Effects in Deep Inelastic Scattering. *Z Phys C* 1989; 43: 625. (b). Lönnblad L, Rapidity gaps and other final state properties in the colour dipole model for deep inelastic scattering. *Z Phys C* 1995; 65: 285.

Received: June 15, 2013

Revised: September 27, 2013

Accepted: October 2, 2013

© Khurelbaatar Begzsuren; Licensee *Bentham Open*.

This is an open access article licensed under the terms of the Creative Commons Attribution Non-Commercial License (<http://creativecommons.org/licenses/by-nc/3.0/>) which permits unrestricted, non-commercial use, distribution and reproduction in any medium, provided the work is properly cited.